Molecular Characterization of the EhaG and UpaG Trimeric Autotransporter Proteins from Pathogenic Escherichia coli

M. Totsika, J. Wells, C. Beloin, J. Valle, L. P. Allsopp, N. P. King, J.-M. Ghigo, M. A. Schembri

Molecular characterisation of the EhaG and UpaG trimeric autotransporter proteins from pathogenic *Escherichia coli*

Makrina Totsika[1], Timothy J. Wells[1], Christophe Beloin[2,3], Jaione Valle[2,4], Luke P Allsopp[1], Nathan P King, Jean-Marc Ghigo[2,3] and Mark A. Schembri[1*]

[1]: *Australian Infectious Disease Research Centre, School of Chemistry and Molecular Biosciences, University of Queensland, Brisbane QLD 4072, Australia.*

[2]: *Institut Pasteur, Unité de Génétique des Biofilms, Département de Microbiologie F-75015 Paris, France.*

[3]: *CNRS, URA2172, F-75015 Paris, France*.

[4]: *current address, Laboratory of Microbial Biofilms, Instituto de Agrobiotecnologia, Universidad Pública de Navarra-CSIC-Gobierno de Navarra, 31006 Pamplona, Spain*.

Running title: EhaG and UpaG TAAs of *E. coli*.

Key words: adhesion, trimeric autotransporter, *Escherichia coli*

* Corresponding author.

Mailing address: School of Chemistry and Molecular Biosciences, Building 76, University of Queensland, Brisbane QLD 4072, Australia. Phone: +617 33653306; Fax: +617 33654699; E-mail: m.schembri@uq.edu.au

Abstract

Trimeric autotransporter proteins (TAAs) are important virulence factors of many Gram-negative bacterial pathogens. A common feature of most TAAs is the ability to mediate adherence to eukaryotic cells or extracellular matrix (ECM) proteins via a cell-surface exposed passenger domain. Here we describe the characterization of EhaG, a TAA identified from enterohaemorrhagic *E. coli* (EHEC) O157:H7. EhaG is a positional orthologue of the recently characterized UpaG TAA from uropathogenic *E. coli* (UPEC). Similar to UpaG, EhaG localized at the bacterial cell surface and promoted cell aggregation, biofilm formation and adherence to a range of ECM proteins. However, the two orthologues display differential cellular binding; EhaG mediates specific adhesion to colorectal epithelial cells while UpaG promotes specific binding to bladder epithelial cells. The EhaG and UpaG TAAs contain extensive sequence divergence in their respective passenger domains that could account for these differences. Indeed, sequence analyses of UpaG and EhaG homologues from several *E. coli* genomes revealed grouping of the proteins in clades almost exclusively represented by distinct *E. coli* pathotypes. The expression of EhaG (in EHEC) and UpaG (in UPEC) was also investigated and shown to be significantly enhanced in a *hns* isogenic mutant, suggesting that H-NS acts as a negative regulator of both TAAs. Thus, while the EhaG and UpaG TAAs contain some conserved binding and regulatory features, they also possess important differences that correlate with the distinct pathogenic lifestyles of EHEC and UPEC.

Introduction

Trimeric autotransporter adhesins (TAAs) are a sub-group of AT proteins that form a stable trimer on the bacterial cell surface (12). TAAs have been identified in a wide range of Gram-negative bacteria and where characterized are universally associated with virulence (30). TAAs are defined by the presence of a short 70-100 amino acid C-terminal membrane anchor domain encoding four β-sheets that forms a trimer to create a full sized β-barrel pore (49). This pore facilities the translocation of the passenger domain to the cell surface (40, 49). This feature of TAAs is different to conventional AT proteins, which possess a translocation domain composed of around 300 amino acids that encode 12-14 aliphatic β-pleated sheets that together form a β-barrel pore (31, 59).

The passenger domain of TAAs requires trimerisation for stability and adhesive activity (11). Modelling of TAAs such as YadA from *Yersinia enterocolitica*, Hia from *Haemophilus influenzae* and BadA *Bartonella henselae* has revealed three distinct regions within the passenger domain; an N-terminal head, a neck and a stalk (35, 50, 60). The N-terminal head structure differs between TAA proteins and is primarily involved in the adhesion properties of the protein (35, 60). The YadA head structure contains single-stranded, left-handed β-helices, the interface of which is formed by periodically occurring, conserved sequence motifs (35). These motifs can be found in the predicted head structures of many TAAs (50).

The head is connected to the stalk by a short, highly conserved sequence (the neck) which functions as an adapter between the large globular head and the narrow stalk domain. The neck is thought to act like a ‘safety pin’, holding the three monomers together, partly explaining the stability of trimeric proteins (35). The stalk domain is repetitive, fibrous and highly divergent in length with its primary function to extend the head domain away from the surface of the bacterium (30). It can however confer other functional properties such as serum resistance (29, 40). The variable number of repeats in the stalk domain can lead to major differences in the size of TAAs. For example, BadA is more than 3,000 amino acids in length (39) while YadA is only 422 amino acids (26). Large TAAs like BadA have intermittent neck domains throughout the long stalk structure (30). The domain build-up of TAA proteins has been demonstrated from the crystal structure of EibD, an immunoglobulin binding TAA protein from *E. coli* (29, 40).

Recently, a TAA from the uropathogenic *E. coli* (UPEC) strain CFT073 was identified (UpaG) that mediates adhesion to human bladder epithelial cells (55). UpaG promotes cell aggregation and biofilm formation on abiotic surfaces by CFT073 and various other UPEC strains as well as binding to the extracellular matrix (ECM) proteins fibronectin and laminin (55). Prevalence studies indicated that *upaG* is frequently associated with extra-intestinal *E. coli* (ExPEC) strains (55). UpaG has also been identified as a potential protective antigen in ExPEC (19).

Enterohemorrhagic *Escherichia coli* (EHEC) are a pathogenic sub-class of diarrheagenic *E. coli* (DEC). Here we identify a TAA from *E. coli* O157:H7, EhaG, which is a positional orthologue of UpaG but contains significant sequence divergence within the passenger-encoding domain. Cloning and expression of the *ehaG* gene from *E. coli* EDL933 revealed the EhaG TAA possesses different functional properties to UpaG. These functional properties correlate with the distinct tissue tropism of EHEC and UPEC pathogens. While UpaG and EhaG displayed different functional characteristics, their expression in UPEC and EHEC is regulated in a common fashion by H-NS.

Materials and Methods

Bacterial strains and growth conditions. The following *E. coli* strains were used in this study: BL21(DE3) (Stratagene), MG1655, MS427 (MG1655*flu*) (38), OS56 (MG1655*flu* gfp^{+}) (48), UPEC CFT073 (33), EHEC EDL933 (37) and CFT073*upaG* (55). Cells were routinely grown at 28^{o}C or 37^{o}C on solid or in liquid lysogeny broth (LB) medium (5), supplemented with the appropriate antibiotics; kanamycin (Kan, 100 µg/ml), chloramphenicol (Cam, 30 µg/ml), ampicillin (Amp, 100 µg/ml). For growth in defined conditions M63B1 supplemented with 0.4% glucose ($M63B1_{Glu}$) media was used as indicated (42).

DNA manipulations and genetic techniques. DNA techniques were performed as previously described (42). Isolation of plasmid DNA was carried out using the QIAprep Spin Miniprep Kit (Qiagen). Restriction endonucleases were used according to the manufacturer's specifications (New England Biolabs). Chromosomal DNA purification was made using the DNeasy Blood and Tissue kit (Qiagen). Oligonucleotides were purchased from Sigma (Australia or France). All polymerase chain reactions requiring proofreading were performed with the Expand High Fidelity Polymerase System (Roche) as described by the manufacturer. Amplified products were sequenced to ensure fidelity of the PCR. DNA sequencing was performed using the ABI Big Dye ver3.1 Kit (ABI) by the Australian Equine Genetics Research Centre, University of Queensland, Brisbane. Prevalence studies for the *upaG* and *ehaG* genes used *Taq* DNA polymerase, as described by the manufacturer (New England Biolabs), with the primers 144 (5'-aatacccagagcattactaacctg) and 145 (5'-accttgtaatttgtagacccaa).

Construction of plasmids. The *ehaG* gene was amplified by PCR from EHEC EDL933 using specific primers designed from the available genome sequence (130: 5'-CGCGCTCGAGATAATAAGGAAcattaatgaacaaaatatttaaag and 131: 5'-CGCGCAAGCTTttaccactgaataccggcaccg). The PCR product was digested with *Xho*I (forward primer) and *Hin*dIII/*Eco*RI (reverse primer) and ligated to *Xho*I-*Hin*dIII/*Eco*RI digested plasmid pBAD/*Myc*-HisA. The resultant plasmid (pOMS01) was then digested with *Eco*RI and ligated with a correspondingly digested kanamycin-resistance encoding gene cassette to give rise to plasmid pEhaG-kan (pOMS15). Resistance to kanamycin was required to facilitate transformation of this plasmid into the *flu*-negative, *gfp*-positive *E. coli* K-12

strain OS56. The *upaG* gene from UPEC CFT073 has been described previously (55). Both genes were cloned using the same strategy, with expression of *ehaG*/*upaG* under control of the arabinose-inducible *araBAD* promoter (24). Neither gene was cloned as a fusion to the 6xHis-encoding sequence of pBAD/*Myc*-HisA.

Construction of mutants. In order to mutate the *ehaG* gene in EDL933 and create a *lacZ* reporter transcriptional fusion in CFT073, we used homologous recombination mediated by λ-red recombinase and either a one-step PCR procedure with 50-bp homology arms for recombination or a three-step PCR procedure with 500-bp homology arms for recombination (7, 14, 15, 52) The primers used to disrupt the *ehaG* gene in EDL933 were 843 (5'-acagctaaagagtcaactgg), 844 (5'-ccatgaggcggcgacgtatcc), 845 (5'-gaagcagctccagcctacactaatgatgctcgctattccttg) and 846 (5'-ctaaggaggatattcatatgtgatccattaagttagtgtgactaagg). The mutation was confirmed using primers 789 (5'-aggacgcccgccataaactg) and 790 (5'-ggtttaacggttgtggacaac) and subsequent sequencing. A *upaG-lacZ* reporter transcriptional fusion in CFT073Δ*lac* was constructed using the same approach but employing primers upaG.lacZzeo.L-5 (cagcttctgcgcttatatcaaggaatagagagcatcaataatgaccatgattacggattc) and upaG.lacZzeo.L-3 (catcaggcaatgtggcgtttacccatttgttaatggatgatcagtcctgctcctcggccac). Mutants were confirmed via PCR and sequencing using primers upaG.ext-5 (aggaattcatcctatgaacc) and upaG.ext-3 (ttatcgttcgaactgctactgtc). CFT073Δ*lac upaG::lacZ-zeo* mutants were screened after mutagenesis with the suicide plasmid pSC189 carrying kanamycin-resistant Mariner transposon described previously (8, 13). Sequencing of the transposon in both directions enabled the identification site of insertion and, hence, the gene disrupted. Mutation of the *hns* gene in EDL933 and CFT073 was performed as previously described (1).

Biofilm assays. Biofilm formation on polystyrene surfaces was monitored by using 96-well microtitre plates (IWAKI) essentially as previously described (46). Briefly, cells were grown for 18 h in LB (containing 0.2% arabinose for induction of AT-encoding genes) at 37^{o}C, washed to remove unbound cells, and stained with crystal violet. Quantification of bound cells was performed by addition of acetone-ethanol (20:80) and measurement of the dissolved crystal violet at an optical density of 590 nm. Flow chamber experiments were performed as previously described (27, 45). Briefly, biofilms were allowed to form on glass surfaces in a multi-channel flow system that permitted continuous monitoring of their structural characteristics. Flow cells were inoculated with OD_{600} = 0.02 standardized cultures pre-

grown overnight in M9 medium containing arabinose and kanamycin. Biofilm development was monitored by confocal scanning laser microscopy at 18 h post inoculation. For analysis of flow cell biofilms, z-stacks were analysed using the COMSTAT software program (25).

Binding to ECM components. Bacterial binding to ECM components was performed in a microtiter plate ELISA assay essentially as previously described (55). Microtiter plates (Maxisorp; Nunc) were coated overnight at 4°C with 2 µg of the following ECM proteins: collagen (types I-V), fibronectin, fibrinogen, laminin, elastin, heparin sulfate, human serum album, BSA (Sigma-Aldrich) or the glycoproteins *N*-acetyl-D-galactosamine (NaGal), *N*-acetyl-D-glucosamine (NaGlu) or *N*-acetylneuraminic acid (NaNa). Wells were washed twice with TBS (137mM NaCl, 10mM Tris, pH 7.4) and then blocked with TBS-2% milk for 1 h. After being washed with TBS, 200 µl of washed and standardized (OD_{600} = 0.1) cultures of *E. coli* strains MS427pEhaG, MS427pUpaG or MS427pBAD was added to 12 replicate wells per ECM component and the plates were incubated at 37°C for 2 h. After being washed to remove non-adherent bacteria, adherent cells were fixed with 4% paraformaldehyde, washed, and incubated for 1 h with anti-*E. coli* serum (Meridian Life Sciences Inc., #B65001R) diluted 1:500 in 0.05% TBS-Tween, 0.2% skim milk, washed and incubated for 1 h with a secondary anti-rabbit conjugated horseradish peroxidase antibody (diluted 1:1000) (Sigma-Aldrich; #A6154). After a final wash adhered bacteria were detected by adding 150 µL of 0.3mg/ml ABTS [2,2´-azino-bis(3-ethylbenzthiazoline-6-sulfonic acid)] Sigma-Aldrich) in 0.1M citric acid pH 4.3, activated with 1 µl/ml 30% hydrogen peroxide] and the absorbance measured at 405 nm.

Epithelial cell binding assays. T24 human bladder carcinoma cells and colorectal epithelial (Caco-2) cells were purchased from the American Type Culture Collection and cultured according to standard protocols. The adherence of MS427pEhaG and MS427pUpaG to cultured T24 or Caco-2 cells was examined essentially as previously described (6, 55). Briefly, wells were seeded with 1.5 x 10^5 epithelial cells in 24-well tissue culture plates and incubated at 37^{o}C in 5% CO_2 until they were confluent. Overnight bacterial cultures were diluted and grown to an OD_{600} = 0.5 in LB with appropriate antibiotics (and 0.2% arabinose for *ehaG*/*upaG* induction). Bacterial cells were washed and added to triplicate epithelial cell monolayers at a multiplicity of infection of 10. Incubation was carried out for 1.5 h at 37°C in 5% CO_2. After incubation, monolayers were washed five times with PBS to remove non-adherent bacteria. The remaining bacteria were then released by eukaryotic cell lysis with

0.1% Triton X-100. The number of adherent bacteria, as well as the inoculating dose, was determined by serial dilution and plating on LB agar. All experiments were performed in triplicate.

Co-infection of Caco-2 epithelial cell monolayers with fluorescently tagged MS427pEhaG and MS427pUpaG was carried out essentially as described above, but with the following modifications. Seeding of epithelial cells was performed in 4-chamber glass culture slides (BD Falcon). The two bacterial strains were mixed at 1:1 ratio and incubated with the Caco-2 cell monolayers for 1.5 h at 37°C in 5% CO_2. Following incubation, monolayers were washed five times with PBS to remove non-adherent bacteria and the adherent bacteria were fixed with 4% paraformaldehyde (PFA). The PFA was then removed by washing with PBS and adherent bacteria were visualised using fluorescence microscopy. Adherent bacteria were counted from 40 fields of view. In these experiments, the level of EhaG and UpaG protein produced by MS427pEhaG and MS427pUpaG, respectively, was similar (data not shown).

Purification of 6xHistidine-tagged EhaG', antibody production and immunoblotting. A 480 bp segment from the passenger-encoding domain of *ehaG* was amplified by PCR with primers 1707 (5'-tacttccaatccaatgcaaacgctattgcgataggtgctg) and 1708 (5'-ttatccacttccaatgttaaagctgtgaaccattaatgg) from *E. coli* EDL933 genomic DNA; underlined nucleotides represent the ligation-independent cloning (LIC) overhangs used for insertion into plasmid pMCSG7 via LIC cloning (16). The resultant plasmid (pEhaGTruncated) contained the base pairs 652-1132 of *ehaG* fused to a 6xHis encoding sequence. *E. coli* BL21 was transformed with plasmid pEhaGTruncated, induced with IPTG and the resultant 6xHis-tagged EhaG truncated protein (containing amino acids 218-378 of EhaG) was assessed by SDS-PAGE analysis as previously described (53). Polyclonal anti-EhaG serum was raised in rabbits by the Institute of Medical and Veterinary Sciences (South Australia). A polyclonal antiserum raised against UpaG has been described previously (55). For immunoblotting, whole-cell lysates were subjected to SDS-PAGE using NuPAGE® Novex® 3-8% Tris-acetate precast gels with NuPAGE® Tris-Acetate running buffer and subsequently transferred to polyvinylidene difluoride (PVDF) microporous membrane filters using the iBlot™ dry blotting system as described by the manufacturer (Invitrogen). EhaG or UpaG rabbit polyclonal antiserum was used as primary and the secondary antibody was alkaline phosphatase-conjugated anti-rabbit IgG. Sigma Fast™ 5-bromo-4-chloro-3-

indolylphosphate–nitroblue tetrazolium (BCIP/NBT) was used as the substrate in the detection process.

β-galactosidase assays. β-galactosidase assays were performed essentially as previously described (32). Briefly, strains carrying *lacZ* fusions were grown on LB plates for 16 h then inoculated into $M63B1_{Glu}$ minimal medium. After 16-18 h of growth the culture was diluted in Z-buffer (60mM Na_2HPO_4, 40mM NaH_2PO_4, 50mM β-mercaptoethanol, 10mM KCl, 1mM $MgSO_4$, pH 7), 0.004% SDS and chloroform was added and the samples were vortexed to permeabilize the cells. Samples were incubated at 28°C and the reaction was initiated by the addition of ONPG. Reactions were stoped with the addition of sodium bicarbonate and the enzymatic activity was assayed in quadruplicate for each strain by measuring the absorbance at 420 nm. Where required, β-galactosidase activity was also observed on LB agar plates containing 5-Bromo-4-chloro-3-indolyl β-D-galactoside (X-gal).

DNA curvature prediction and electrophoretic mobility shift assays. The *upaG* promoter region was analysed *in silico* using Bendit, a program that enables the prediction of a curvature-propensity plot calculated with DNase I-based parameters (http://hydra.icgeb.trieste.it/dna/) (56). The curvature is calculated as a vector sum of dinucleotide geometries (roll, tilt and twist angles) and expressed as degrees per helical turn (10.5°/helical turn = 1°/bp). Experimentally tested curved motifs produce curvature values of 5-25°/helical turn, whereas straight motifs give values below 5°/helical turn. The 250 bp *upaG* promoter region was amplified using primers upaG-250-5 (ttagcaaaatggcagcaatt) and upaG+1-3 (tattgatgctctctattcct) and its intrinsic curvature assessed by comparing its electrophoretic mobility with that of an unbent marker fragment (Promega 100 bp DNA ladder) on a 0.5% TBE, 7.5% PAGE gel at 4°C for retarded gel electrophoretic mobility.

Gel shift assays were performed essentially as previously described (4). A DNA mixture comprising the PCR amplified *upaG* promoter region and TaqI-SspI digested pBR322 at equimolar ratio was incubated at room temperature for 15 minutes with increasing amounts of native purified H-NS protein (a gift from Dr S. Rimsky) in 30 µl of reaction mixture containing 40mM Hepes pH 8, 60mM potassium glutamate, 8mM magnesium aspartate, 5mM dithiothreitol, 10% glycerol, 0.1% octylphenoxypolyethoxyethanol, 0.1mg/ml BSA (H-NS binding buffer). DNA fragments and DNA-protein complexes were resolved by gel

electrophoresis (0.5% TBE, 3% MS agarose gel run at 50 V at 4°C) and visualized after staining with ethidium bromide.

Results

Sequence variation in *E. coli* UpaG homologues correlates with strain pathotype. We used the translated amino acid sequence of *upaG* to probe all protein sequences encoded in 28 *E. coli* genomes available in the NCBI database (Table S1). An intact gene encoding a putative TAA was found in 24 of the 28 genomes at the same genomic location as *upaG* in CFT073. Interestingly, three of the *E. coli* strains lacking the gene were commensal strains (ATCC8739, K-12 MG1655 and W3110). Enteropathogenic *E. coli* (EPEC) strain E2348/69 contains a truncated gene due to a frameshift mutation. Multiple alignment of the 24 putative TAA protein sequences revealed that the signal sequence and translocation domain are highly conserved, while the passenger domain is highly variable (Fig. 1A). The passenger domain of all sequences contained Hep_Hag and HIM motifs, however diversity was observed in both motif sequence and number (Fig 1A). Phylogenetic analysis of the 24 translated full-length protein sequences revealed grouping according to strain pathotype, with sequences from DEC strains clading separately from those encoded in ExPEC strains (Fig 1B). Proteins belonging to DEC strains shared high sequence identity (95%), while proteins encoded in ExPEC genomes shared 53% sequence identity, significantly higher than the overall 38% identity shared among the 24 *E. coli* TAA proteins examined.

***upaG* is highly prevalent among diarrheagenic *E. coli*.** We have previously demonstrated that *upaG* is commonly found in UPEC isolates (55). However, the primers used in our previous molecular screening were designed to amplify sequence from the passenger domain of *upaG* that is not conserved among the gene homologues found in the genome of DEC strains. In order to determine the prevalence of *upaG* homologues in DEC strains, we designed a new set of primers specific to a highly conserved region within the translocation domain and screened a collection of Shiga toxin-producing *E. coli* (STEC) isolates. We also screened a collection of UPEC isolates with the new set of primers. A product of the correct size was found in 92% (51/55) of STEC and 86.5% (64/74) of UPEC strains, indicating that *upaG* homologues are highly prevalent among pathogenic *E. coli* of intestinal as well as extraintestinal origin.

Comparative sequence analysis of UpaG and EhaG from prototypic strains UPEC CFT073 and EHEC EDL933, respectively. We hypothesized that the pathotype-specific grouping of UpaG homologues, due to the variable sequence of the function-encoding

passenger domain, suggests that TAA proteins may have evolved specificity for their host environment. To test this tenet, we selected one representative protein from the ExPEC group and one from the DEC clade to perform a detailed comparative sequence and functional analysis. UpaG from the prototypic UPEC strain CFT073 was chosen as the only functionally characterized TAA member from *E. coli* and was compared to its positional orthologue in the prototypic EHEC strain EDL933 (gene z5029). The z5029 gene was named *ehaG*, in a fashion consistent with previously characterized AT proteins from EHEC (57) while still acknowledging that it is a positional orthologue of *upaG* from UPEC. The *ehaG* gene (4767bp) encodes a protein similar to UpaG, containing an extended N-terminal signal sequence with predicted cleavage after amino acid 53, as well as an 89 amino acid C-terminal translocation domain conserved among all TAA adhesins (Fig 2A). Despite being positional orthologues, *upaG* and *ehaG* differ significantly in size and sequence (Fig 2A). The predicted proteins are 1778 and 1588 amino acids, respectively, with the difference due to the presence of 190 additional amino acids in the passenger domain of UpaG (Fig. 2A). In fact, although their translocation domains are 100% identical, the two proteins share only 65% identity over the passenger domain. Sequence analysis of the passenger domain of EhaG and UpaG against the Pfam and TIGRFAM databases showed that the proteins contain 13 and 14 Hep_Hag repeats, respectively. The majority of these 28 amino acid long repeats are found sequentially at the N-terminal end of the passenger domain (Fig 2A). The head crystal structure of TAAs YadA and BadA are composed of such domains (35, 50) and it is likely that this region encodes the head of the EhaG and UpaG proteins (Fig 2A). This is also supported by domain annotation for UpaG and EhaG proteins performed using the daTAA server (50) (data not shown). EhaG and UpaG also encode 12 and 15 HIM motifs, respectively, dispersed along the passenger domain. This highly conserved 24 amino acid motif is known to form the neck-structure in YadA (35), a transition region between the globular head and the narrower stalk domain of the protein. Alignment of the multiple Hep_Hag and HIM sequences present in EhaG and UpaG (Fig 2B) revealed that HIM sequences are well conserved between the two homologues, whereas the Hep_Hag sequences displayed some degree of variability (Fig 2B and C).

EhaG from EHEC EDL933 mediates autoaggregation and biofilm formation. The significant sequence differences in the passenger domain of EhaG and UpaG prompted us to investigate whether EhaG possesses the same functional properties as UpaG. For this purpose

317 the *ehaG* gene was amplified from the chromosome of EDL933 and cloned into
318 pBAD/MycHis-A under the control of the inducible *araBAD* promoter (24). The pEhaG
319 vector was introduced into the previously described *E. coli flu* mutant strain MS427 (38) that
320 is deficient in Ag43 expression and thus lacks the ability to autoaggregate and form a biofilm.
321 Over-expression of EhaG in this background resulted in cell-cell aggregation from standing
322 overnight cultures within 20 minutes, in contrast to the MS427pBAD control (Fig 3A). We
323 also tested the ability of EhaG to mediate biofilm formation in two distinct systems. In the
324 polystyrene microtitre plate assay MS427pEhaG formed a significant biofilm compared to
325 the MS427pBAD control following induction with arabinose ($P<0.001$; Fig 3B). To compare
326 the biofilm forming capacity of EhaG and UpaG, we used the dynamic model of a
327 continuous-flow chamber. Green fluorescent protein (GFP)-tagged MS427 cells (OS56)
328 expressing *ehaG* from plasmid pEhaG or *upaG* from plasmid pUpaG were monitored for
329 biofilm formation over 18 hours using confocal laser scanning microscopy. In contrast to the
330 OS56pBAD control, cells producing either EhaG or UpaG formed a strong biofilm across the
331 entire surface of the chamber to a depth of approximately 15µm (Fig 3C).

332 **EhaG and UpaG bind to extracellular matrix (ECM) proteins.** A common feature of
333 TAAs is the ability to mediate binding to components of the ECM such as collagen and
334 laminin. We therefore examined the ability of EhaG and UpaG to bind to a range of ECM
335 proteins. The MS427pEhaG and MS427pUpaG strains both displayed binding to laminin,
336 fibronectin, fibrinogen and collagen types I, II, III and V (Fig 4). In contrast, no UpaG/EhaG-
337 mediated binding was observed to type IV collagen, elastin, heparin sulfate, human serum
338 albumin, bovine serum albumin or the glycans *N*-acetyl-D-galactosamine (NaGal), *N*-acetyl-
339 D-glucosamine (NaGlu) and *N*-acetylneuraminic acid (NaNa) (Fig 4 and data not shown).
340 Thus, EhaG and UpaG mediate binding to selected ECM proteins, and the binding specificity
341 to these ECM proteins is conserved between both TAAs.

342 **EhaG and UpaG mediate differential cellular adhesion.** All TAAs characterized to date
343 play a role in adhesion. We have previously demonstrated that UpaG enhances adhesion of
344 CFT073 to T24 bladder epithelial cells (55). We therefore investigated if EhaG has a similar
345 function; however no increase was observed in the number of adherent bacteria recovered
346 from T24 bladder epithelial cell monolayers infected with EhaG-producing MS427 cells
347 compared to MS427pBAD (data not shown). Since EhaG is encoded by an enteric pathogen,
348 we therefore tested its ability to mediate binding to intestinal epithelial cells. The number of

adherent bacteria recovered after incubation of Caco-2 epithelial cell monolayers with MS427pEhaG was significantly higher than the MS427pBAD control (Fig 5A). The ability of EhaG to mediate bacterial adhesion to intestinal epithelial cells prompted us to investigate if UpaG can also mediate adhesion to Caco-2 cells. MS427pUpaG failed to adhere to Caco-2 epithelial cell monolayers at significantly higher numbers than the MS427pBAD control (Fig 5A). Upon co-infection of Caco-2 epithelial cell monolayers with a mixed (1:1) population of EhaG- and UpaG-producing MS427 cells that carried different fluorescent chromosomal markers (green for MS427pEhaG and red for MS427pUpaG), EhaG-producing cells adhered at 2.5-fold greater numbers than UpaG-producing cells (Fig 5B and C). Reverse competition experiments using red MS427pEhaG and green MS427pUpaG cells produced a similar result (data not shown), ruling out a potential fluorophore-dependent bias in bacterial numbers.

Regulation of *upaG* expression by H-NS. We did not detect expression of UpaG or EhaG in protein samples prepared from *in vitro* cultured UPEC CFT073 and EHEC EDL933, respectively, using western blotting with specific polyclonal antiserum (data not shown) (55). To explore possible reasons for this lack of expression, we constructed a *lacZ* reporter fusion to the chromosomal promoter of *upaG* in CFT073 (CFT073Δ*lac_upaG*::*lacZ*) and subjected the strain to random mariner-transposon mutagenesis in order to identify negative regulators of *upaG* expression. Screening of 20,000 mutants identified two mutants with β-galactosidase activity. Both mutants carried transposon insertions in different positions of the gene encoding the global regulator H-NS (corresponding to amino acid positions 97 and 127 of the H-NS protein). To confirm the regulatory role of H-NS in expression of *upaG*, we constructed a *hns* deletion in CFT073Δ*lac_upaG*::*lacZ* and subsequently complemented this strain with a plasmid containing the *hns* gene downstream of the inducible *araBAD* promoter. Relative β-galactosidase activity was measured in $M63B1_{Glu}$ grown cultures of CFT073Δ*lac_upaG*::lacZ_Δ*hns* complemented with empty pBAD30 vector or pBAD30*hns* in the absence or presence of 0.2% arabinose. Deletion of *hns* in CFT073 de-repressed *upaG* expression by six-fold, which was reversed upon complementation with pBAD30*hns* but not the pBAD30 control under arabinose induction (Fig 6A).

H-NS binds to the *upaG* promoter region. H-NS has an affinity for AT rich, intrinsically curved double-stranded DNA. The 250 bp promoter region of *upaG* is 60.4% AT rich and we examined its properties as well as its H-NS binding capacity using several approaches. First, we generated an *in silico* curvature-propensity plot calculated with DNase I-based parameters

and showed that this 250 bp segment may adopt a curved conformation (Fig 6B). Next, we demonstrated this curvature experimentally by examination of the PCR amplified 250 bp fragment using polyacrylamide gel electrophoresis at 4°C. Using this method, which has been used previously to demonstrate DNA curvature (54, 58), the 250 bp *upaG* promoter region displayed a slightly retarded gel electrophoretic mobility compared to non-curved DNA standards (Fig 6C). Finally, to demonstrate direct binding of H-NS to the 250 bp promoter region of *upaG*, we performed electrophoretic mobility shift assays. The 250 bp PCR product was mixed with *Taq*I-*Ssp*I-digested pBR322 DNA (which contains the *bla* promoter and has been previously shown to be bound by H-NS), incubated with increasing concentrations of purified H-NS protein and subsequently visualized by gel electrophoresis. The 250 bp *upaG* promoter region and the fragment containing the *bla*-promoter were retarded in mobility by the addition of 0.5 μM H-NS (Fig 6D). The pBR322 fragments not containing the *bla*-promoter were not influenced by H-NS at these concentrations, indicating that H-NS binds with specificity. These results suggest that H-NS binds to the regulatory region of *upaG* by recognizing a DNA region within 250 bp 5′ of the ATG translation start codon.

Mutation of the *hns* gene results in increased expression of *upaG* and *ehaG*. To confirm that H-NS acts as a repressor of *upaG* expression, we constructed a *hns* isogenic mutant in CFT073 and examined UpaG production by Western blot analysis. Loss of H-NS in CFT073 resulted in an increase in the production of UpaG that was detectable by western blot analysis using an anti-UpaG specific serum (Fig 7A). We also constructed an isogenic EDL933 *hns* mutant strain and tested for EhaG expression by western blot analysis using an anti-EhaG specific serum. Similar to CFT073, deletion of *hns* in EDL933 result in increased expression of the EhaG protein (Fig 7B). Taken together, these results demonstrate that H-NS negatively regulates the expression of *upaG* in CFT073 and *ehaG* in EDL933.

Discussion

TAAs are an important group of virulence factors in many Gram-negative pathogens. TAAs are translocated to the cell surface via the type V secretion pathway and adopt a trimeric conformation in the outer membrane. Three TAAs have been characterized from pathogenic *E. coli*, namely UpaG, Saa and the Eib group of proteins (36, 43, 55). Here we have characterised the EhaG protein, a TAA from enterohaemorrhagic *E. coli* O157:H7. Like its

positional orthologue UpaG from UPEC, EhaG mediates bacterial cell aggregation, biofilm formation and adherence to ECM proteins. However, in contrast to UpaG (which mediates specific adherence to bladder epithelial cells), EhaG mediates specific adherence to intestinal epithelial cells.

EhaG and UpaG both possess a classical TAA domain structure consisting of an N-terminal signal sequence, a passenger domain and a C-terminal translocation domain. The translocation domain is the most conserved feature of the TAA family, with the 70-100 amino acid C-terminal region responsible for translocation of the passenger domain to the bacterial surface in all TAAs (40). We showed previously that the last 71 amino acids of UpaG, corresponding to the L1-β subdomain, represent the translocation unit (55). This region is completely conserved at the amino acid level in EhaG and UpaG.

In contrast to the translocation domain, the passenger domain of EhaG and UpaG exhibits extensive amino acid sequence variability (65% identity). Further analysis of the passenger domain revealed that the Hep_Hag motifs in the predicted head region were more variable than the HIM motifs in the stalk and neck structures. The head region has been found to be responsible for adhesion in other TAAs (30). Although the structural domains responsible for the binding properties of EhaG and UpaG have not been defined, it is likely that sequence differences in the head region account for the different EhaG and UpaG cell adherence phenotypes observed in this study.

Most trimeric AT proteins characterised to-date display an adhesive activity mediating bacterial interactions with either host cells or ECM proteins (3, 9, 10, 23, 41, 44). Both EhaG and UpaG possessed several conserved features - they mediated cell aggregation, biofilm formation and adhesion to laminin, fibronectin, fibrinogen and collagen types I, II, III and V. There are several features of both proteins that could account for these observations. The multiple Hep_Hag motifs in the head region, despite a degree of sequence variation, could mediate some of these functions. Alternatively, these properties may be associated with conserved structural features of both proteins rather than the presence of specific binding domains.

We found that the sequence divergence in the passenger domain of EhaG and UpaG corresponded strongly with diarrheagenic and extraintestinal *E. coli* pathotypes. In the case of DEC strains, EhaG is highly conserved and exhibits >95% amino acid identity. In contrast,

the sequence of UpaG among ExPEC strains was more variable. The UpaG protein from UPEC CFT073 has previously been shown to mediate cell aggregation, biofilm formation and adhesion to the ECM proteins laminin and fibronectin (55). The extensive sequence variation of UpaG suggests that there may be differences in these functional properties between UpaG variants from different UPEC/ExPEC strains. Thus, a more detailed analysis of the functions of different UpaG variants is required to properly assess its role in virulence.

Adherence of EHEC to the intestinal epithelium is essential for initiation of infection. The adherence of *E. coli* O157:H7 to Caco-2 cells has been shown to proceed in two stages; an initial diffuse adherence to epithelial cells followed by proliferation to develop micro-colonies and intimate adherence (51). The intimate attachment and micro-colony formation are thought to be mediated primarily by intimin-Tir interactions whereas the diffuse adherence to Caco-2 cells requires multiple factors encoded by the LEE and additional chromosomal loci (51). Some of the proteins implicated in this initial adherence include ToxB and EspA (20, 51). The diffuse adherence pattern mediated by EhaG to Caco-2 cells following expression in *E. coli* K-12 suggests it may contribute to initial adherence of *E. coli* O157:H7 to intestinal epithelial cells. This remains to be demonstrated.

Immunodetection employing antibodies specific to EhaG and UpaG failed to detect these proteins in whole cell extracts prepared from wild-type strains EDL933 and CFT073, respectively. We were also unable to detect expression of EhaG or UpaG from wild-type bacteria during interaction with cultured epithelial cells (data not shown). This prompted us to examine possible mechanisms by which the expression of *ehaG* and *upaG* could be repressed. We initially focused our analysis on *upaG* and identified a role for H-NS in its regulation. At the transcriptional level, a significant increase in *upaG* promoter activity was observed in a CFT073Δ*lac_upaG*::*lacZ-zeo hns* mutant. Consistent with this result, we also observed an increase in the expression of the UpaG protein by CFT073 in a *hns* mutant background. H-NS is a histone-like DNA-binding protein that shows affinity for A-T rich and bent nucleation sites on DNA (17, 18). Our data demonstrates that H-NS acts as a repressor of *upaG* transcription, most likely through direct binding to a region comprising the 250 bp upstream of the *upaG* open-reading frame. This sequence shares 83% nucleotide sequence conservation with the corresponding region in *ehaG*; indeed we also observed an increase in the expression of EhaG by EDL933 in a *hns* mutant background. Thus, the transcription of *ehaG* and *upaG* is negatively regulated by H-NS. It is possible that the transcription of *ehaG*

(in EHEC) and *upaG* (in UPEC) is coordinated with other H-NS repressed genes. For example, mutation of the *hns* gene in UPEC strain 536 results in the de-repression of multiple virulence factors including alpha-hemolysin, iron uptake systems and fimbriae (34), and several cryptic *E. coli* chaperone-usher fimbrial genes have also been shown to be repressed by H-NS in *E. coli* (28). The binding of H-NS to DNA is also modulated by temperature, with relief of repression for many genes observed above a threshold temperature of 32^{o}C (18). Although we did not observe expression of EhaG/UpaG at 37^{o}C in our experiments, it is possible that these proteins are expressed under specific conditions such as during host infection.

In this study we have examined the functional properties of the trimeric autotransporter EhaG from EHEC, and compared its characteristics to UpaG from UPEC. Both proteins share several conserved features, yet also possess unique properties that may be associated with host tissue tropism and pathogenesis. One property common to EhaG and UpaG is the ability to mediate biofilm formation. The role of biofilm formation in chronic bladder infection by UPEC (2) and environmental contamination of food by EHEC (47) has been documented. Indeed, given the recent outbreak of the STEC O104 strain in Germany, it will be important to thoroughly characterize the role of proteins such as EhaG in biofilm growth by pathogenic *E. coli*.

Acknowledgements:

We thank Dr Sylvie Rimsky for providing the purified native H-NS protein. This work was supported by grants from the Australian National Health and Medical Research Council (631654), the Australian Research Council (DP1097032), the University of Queensland (ECR grant to MT), the Institut Pasteur, the CNRS URA 2172, the Network of Excellence EuroPathoGenomics, the European Community (LSHB-CT-2005-512061). MAS is supported by an ARC Future Fellowship (FT100100662) and JV was a Marie-Curie Fellow.

References

1. **Allsopp, L. P., C. Beloin, G. C. Ulett, J. Valle, M. Totsika, O. Sherlock, J. M. Ghigo, and M. A. Schembri.** 2011. Molecular Characterization of UpaB and UpaC - two new Autotransporter Proteins of Uropathogenic Escherichia coli CFT073. Infect Immun.
2. **Anderson, G. G., J. J. Palermo, J. D. Schilling, R. Roth, J. Heuser, and S. J. Hultgren.** 2003. Intracellular bacterial biofilm-like pods in urinary tract infections. Science **301:**105-107.
3. **Barenkamp, S. J.** 1996. Immunization with high-molecular-weight adhesion proteins of nontypeable Haemophilus influenzae modifies experimental otitis media in chinchillas. Infect Immun **64:**1246-1251.
4. **Beloin, C., and C. J. Dorman.** 2003. An extended role for the nucleoid structuring protein H-NS in the virulence gene regulatory cascade of Shigella flexneri. Mol Microbiol **47:**825-838.
5. **Bertani, G.** 1951. Studies on lysogenesis. I. The mode of phage liberation by lysogenic Escherichia coli. J Bacteriol **62:**293-300.
6. **Bokil, N. J., M. Totsika, A. J. Carey, K. J. Stacey, V. Hancock, B. M. Saunders, T. Ravasi, G. C. Ulett, M. A. Schembri, and M. J. Sweet.** 2011. Intramacrophage survival of uropathogenic Escherichia coli: differences between diverse clinical isolates and between mouse and human macrophages. Immunobiology **216:**1164-1171.
7. **Chaveroche, M. K., J. M. Ghigo, and C. d'Enfert.** 2000. A rapid method for efficient gene replacement in the filamentous fungus Aspergillus nidulans. Nucleic Acids Res **28:**E97.
8. **Chiang, S. L., and E. J. Rubin.** 2002. Construction of a mariner-based transposon for epitope-tagging and genomic targeting. Gene **296:**179-185.
9. **Comanducci, M., S. Bambini, B. Brunelli, J. Adu-Bobie, B. Arico, B. Capecchi, M. M. Giuliani, V. Masignani, L. Santini, S. Savino, D. M. Granoff, D. A. Caugant, M. Pizza, R. Rappuoli, and M. Mora.** 2002. NadA, a novel vaccine candidate of Neisseria meningitidis. J Exp Med **195:**1445-1454.
10. **Cope, L. D., E. R. Lafontaine, C. A. Slaughter, C. A. Hasemann, Jr., C. Aebi, F. W. Henderson, G. H. McCracken, Jr., and E. J. Hansen.** 1999. Characterization of the Moraxella catarrhalis uspA1 and uspA2 genes and their encoded products. J Bacteriol **181:**4026-4034.
11. **Cotter, S. E., N. K. Surana, S. Grass, and J. W. St Geme, 3rd.** 2006. Trimeric autotransporters require trimerization of the passenger domain for stability and adhesive activity. J Bacteriol **188:**5400-5407.
12. **Cotter, S. E., N. K. Surana, and J. W. St Geme, 3rd.** 2005. Trimeric autotransporters: a distinct subfamily of autotransporter proteins. Trends Microbiol **13:**199-205.
13. **Da Re, S., and J. M. Ghigo.** 2006. A CsgD-independent pathway for cellulose production and biofilm formation in Escherichia coli. J Bacteriol **188:**3073-3087.
14. **Datsenko, K. A., and B. L. Wanner.** 2000. One-step inactivation of chromosomal genes in Escherichia coli K-12 using PCR products. Proc Natl Acad Sci U S A **97:**6640-6645.
15. **Derbise, A., B. Lesic, D. Dacheux, J. M. Ghigo, and E. Carniel.** 2003. A rapid and simple method for inactivating chromosomal genes in Yersinia. FEMS Immunol Med Microbiol **38:**113-116.

16. **Donnelly, M. I., M. Zhou, C. S. Millard, S. Clancy, L. Stols, W. H. Eschenfeldt, F. R. Collart, and A. Joachimiak.** 2006. An expression vector tailored for large-scale, high-throughput purification of recombinant proteins. Protein Expr Purif **47:**446-454.
17. **Dorman, C. J.** 2007. H-NS, the genome sentinel. Nat Rev Microbiol **5:**157-161.
18. **Dorman, C. J.** 2004. H-NS: a universal regulator for a dynamic genome. Nat Rev Microbiol **2:**391-400.
19. **Durant, L., A. Metais, C. Soulama-Mouze, J. M. Genevard, X. Nassif, and S. Escaich.** 2007. Identification of candidates for a subunit vaccine against extraintestinal pathogenic Escherichia coli. Infect Immun **75:**1916-1925.
20. **Ebel, F., T. Podzadel, M. Rohde, A. U. Kresse, S. Kramer, C. Deibel, C. A. Guzman, and T. Chakraborty.** 1998. Initial binding of Shiga toxin-producing Escherichia coli to host cells and subsequent induction of actin rearrangements depend on filamentous EspA-containing surface appendages. Mol Microbiol **30:**147-161.
21. **Felsenstein, J.** 2005. PHYLIP (Phylogeny Inference Package) version 3.6. Distributed by the author. Department of Genome Science, University of Washington, Seattle.
22. **Finn, R. D., J. Mistry, J. Tate, P. Coggill, A. Heger, J. E. Pollington, O. L. Gavin, P. Gunasekaran, G. Ceric, K. Forslund, L. Holm, E. L. L. Sonnhammer, S. R. Eddy, and A. Bateman.** 2010. The Pfam protein families database. Nucleic Acids Research **38:**D211-D222.
23. **Geme, J. W., 3rd, and D. Cutter.** 1995. Evidence that surface fibrils expressed by Haemophilus influenzae type b promote attachment to human epithelial cells. Mol Microbiol **15:**77-85.
24. **Guzman, L. M., D. Belin, M. J. Carson, and J. Beckwith.** 1995. Tight regulation, modulation, and high-level expression by vectors containing the arabinose PBAD promoter. J Bacteriol **177:**4121-4130.
25. **Heydorn, A., A. T. Nielsen, M. Hentzer, C. Sternberg, M. Givskov, B. K. Ersboll, and S. Molin.** 2000. Quantification of biofilm structures by the novel computer program COMSTAT. Microbiology **146 (Pt 10):**2395-2407.
26. **Hoiczyk, E., A. Roggenkamp, M. Reichenbecher, A. Lupas, and J. Heesemann.** 2000. Structure and sequence analysis of Yersinia YadA and Moraxella UspAs reveal a novel class of adhesins. Embo J **19:**5989-5999.
27. **Kjaergaard, K., M. A. Schembri, C. Ramos, S. Molin, and P. Klemm.** 2000. Antigen 43 facilitates formation of multispecies biofilms. Environ Microbiol **2:**695-702.
28. **Korea, C. G., R. Badouraly, M. C. Prevost, J. M. Ghigo, and C. Beloin.** 2010. Escherichia coli K-12 possesses multiple cryptic but functional chaperone-usher fimbriae with distinct surface specificities. Environ Microbiol **12:**1957-1977.
29. **Leo, J. C., A. Lyskowski, K. Hattula, M. D. Hartmann, H. Schwarz, S. J. Butcher, D. Linke, A. N. Lupas, and A. Goldman.** 2011. The Structure of E. coli IgG-Binding Protein D Suggests a General Model for Bending and Binding in Trimeric Autotransporter Adhesins. Structure **19:**1021-1030.
30. **Linke, D., T. Riess, I. B. Autenrieth, A. Lupas, and V. A. Kempf.** 2006. Trimeric autotransporter adhesins: variable structure, common function. Trends Microbiol **14:**264-270.
31. **Loveless, B. J., and M. H. Saier, Jr.** 1997. A novel family of channel-forming, autotransporting, bacterial virulence factors. Mol Membr Biol **14:**113-123.

32. **Miller, J. H.** 1992. A Short Course in Bacterial Genetics: A Laboratory Manual and Handbook for *Escherichia coli* and Related Bacteria. Cold Spring Harbor, NY, USA: Cold Spring Harbor Laboratory Press.
33. **Mobley, H. L., D. M. Green, A. L. Trifillis, D. E. Johnson, G. R. Chippendale, C. V. Lockatell, B. D. Jones, and J. W. Warren.** 1990. Pyelonephritogenic Escherichia coli and killing of cultured human renal proximal tubular epithelial cells: role of hemolysin in some strains. Infect Immun **58:**1281-1289.
34. **Muller, C. M., U. Dobrindt, G. Nagy, L. Emody, B. E. Uhlin, and J. Hacker.** 2006. Role of histone-like proteins H-NS and StpA in expression of virulence determinants of uropathogenic Escherichia coli. J Bacteriol **188:**5428-5438.
35. **Nummelin, H., M. C. Merckel, Y. el Tahir, P. Ollikka, M. Skurnik, and A. Goldman.** 2003. Structural studies of Yersinia adhesin YadA. Adv Exp Med Biol **529:**85-88.
36. **Paton, A. W., P. Srimanote, M. C. Woodrow, and J. C. Paton.** 2001. Characterization of Saa, a novel autoagglutinating adhesin produced by locus of enterocyte effacement-negative Shiga-toxigenic Escherichia coli strains that are virulent for humans. Infect Immun **69:**6999-7009.
37. **Perna, N. T., G. Plunkett, 3rd, V. Burland, B. Mau, J. D. Glasner, D. J. Rose, G. F. Mayhew, P. S. Evans, J. Gregor, H. A. Kirkpatrick, G. Posfai, J. Hackett, S. Klink, A. Boutin, Y. Shao, L. Miller, E. J. Grotbeck, N. W. Davis, A. Lim, E. T. Dimalanta, K. D. Potamousis, J. Apodaca, T. S. Anantharaman, J. Lin, G. Yen, D. C. Schwartz, R. A. Welch, and F. R. Blattner.** 2001. Genome sequence of enterohaemorrhagic Escherichia coli O157:H7. Nature **409:**529-533.
38. **Reisner, A., J. A. Haagensen, M. A. Schembri, E. L. Zechner, and S. Molin.** 2003. Development and maturation of Escherichia coli K-12 biofilms. Mol Microbiol **48:**933-946.
39. **Riess, T., S. G. Andersson, A. Lupas, M. Schaller, A. Schafer, P. Kyme, J. Martin, J. H. Walzlein, U. Ehehalt, H. Lindroos, M. Schirle, A. Nordheim, I. B. Autenrieth, and V. A. Kempf.** 2004. Bartonella adhesin a mediates a proangiogenic host cell response. J Exp Med **200:**1267-1278.
40. **Roggenkamp, A., N. Ackermann, C. A. Jacobi, K. Truelzsch, H. Hoffmann, and J. Heesemann.** 2003. Molecular analysis of transport and oligomerization of the Yersinia enterocolitica adhesin YadA. J Bacteriol **185:**3735-3744.
41. **Roggenkamp, A., H. R. Neuberger, A. Flugel, T. Schmoll, and J. Heesemann.** 1995. Substitution of two histidine residues in YadA protein of Yersinia enterocolitica abrogates collagen binding, cell adherence and mouse virulence. Mol Microbiol **16:**1207-1219.
42. **Sambrook, J., E. F. Fritsch, and M. T.** 1989. Molecular cloning: a laboratory manual. 2nd ed. Cold Spring Harbor Laboratory Press, Cold Spring Harbor, N.Y.
43. **Sandt, C. H., Y. D. Wang, R. A. Wilson, and C. W. Hill.** 1997. Escherichia coli strains with nonimmune immunoglobulin-binding activity. Infect Immun **65:**4572-4579.
44. **Scarselli, M., D. Serruto, P. Montanari, B. Capecchi, J. Adu-Bobie, D. Veggi, R. Rappuoli, M. Pizza, and B. Arico.** 2006. Neisseria meningitidis NhhA is a multifunctional trimeric autotransporter adhesin. Mol Microbiol **61:**631-644.
45. **Schembri, M. A., K. Kjaergaard, and P. Klemm.** 2003. Global gene expression in Escherichia coli biofilms. Mol Microbiol **48:**253-267.

46. **Schembri, M. A., and P. Klemm.** 2001. Biofilm formation in a hydrodynamic environment by novel fimh variants and ramifications for virulence. Infect Immun **69:**1322-1328.
47. **Seo, K. H., and J. F. Frank.** 1999. Attachment of Escherichia coli O157:H7 to lettuce leaf surface and bacterial viability in response to chlorine treatment as demonstrated by using confocal scanning laser microscopy. J Food Prot **62:**3-9.
48. **Sherlock, O., M. A. Schembri, A. Reisner, and P. Klemm.** 2004. Novel roles for the AIDA adhesin from diarrheagenic Escherichia coli: cell aggregation and biofilm formation. J Bacteriol **186:**8058-8065.
49. **Surana, N. K., D. Cutter, S. J. Barenkamp, and J. W. St Geme, 3rd.** 2004. The Haemophilus influenzae Hia autotransporter contains an unusually short trimeric translocator domain. J Biol Chem **279:**14679-14685.
50. **Szczesny, P., and A. Lupas.** 2008. Domain annotation of trimeric autotransporter adhesins--daTAA. Bioinformatics **24:**1251-1256.
51. **Tatsuno, I., H. Kimura, A. Okutani, K. Kanamaru, H. Abe, S. Nagai, K. Makino, H. Shinagawa, M. Yoshida, K. Sato, J. Nakamoto, T. Tobe, and C. Sasakawa.** 2000. Isolation and characterization of mini-Tn5Km2 insertion mutants of enterohemorrhagic Escherichia coli O157:H7 deficient in adherence to Caco-2 cells. Infect Immun **68:**5943-5952.
52. **Ulett, G. C., J. Valle, C. Beloin, O. Sherlock, J. M. Ghigo, and M. A. Schembri.** 2007. Functional analysis of antigen 43 in uropathogenic Escherichia coli reveals a role in long-term persistence in the urinary tract. Infect Immun **75:**3233-3244.
53. **Ulett, G. C., R. I. Webb, and M. A. Schembri.** 2006. Antigen-43-mediated autoaggregation impairs motility in Escherichia coli. Microbiology **152:**2101-2110.
54. **Ussery, D. W., C. F. Higgins, and A. Bolshoy.** 1999. Environmental influences on DNA curvature. J Biomol Struct Dyn **16:**811-823.
55. **Valle, J., A. N. Mabbett, G. C. Ulett, A. Toledo-Arana, K. Wecker, M. Totsika, M. A. Schembri, J. M. Ghigo, and C. Beloin.** 2008. UpaG, a new member of the trimeric autotransporter family of adhesins in uropathogenic Escherichia coli. J Bacteriol **190:**4147-4161.
56. **Vlahovicek, K., L. Kajan, and S. Pongor.** 2003. DNA analysis servers: plot.it, bend.it, model.it and IS. Nucleic Acids Res **31:**3686-3687.
57. **Wells, T. J., J. J. Tree, G. C. Ulett, and M. A. Schembri.** 2007. Autotransporter proteins: novel targets at the bacterial cell surface. FEMS Microbiol Lett **274:**163-172.
58. **Yamada, H., S. Muramatsu, and T. Mizuno.** 1990. An Escherichia coli protein that preferentially binds to sharply curved DNA. J Biochem **108:**420-425.
59. **Yen, M. R., C. R. Peabody, S. M. Partovi, Y. Zhai, Y. H. Tseng, and M. H. Saier.** 2002. Protein-translocating outer membrane porins of Gram-negative bacteria. Biochim Biophys Acta **1562:**6-31.
60. **Yeo, H. J., S. E. Cotter, S. Laarmann, T. Juehne, J. W. St Geme, 3rd, and G. Waksman.** 2004. Structural basis for host recognition by the Haemophilus influenzae Hia autotransporter. Embo J **23:**1245-1256.

Figure legends

Fig 1. Sequence analysis of UpaG homologues from 24 *E. coli* genomes available on the NCBI database and listed in Table S1. (A) Similarity plot of 24 UpaG translated amino acid sequences aligned using Clustal W. High sequence conservation (indicated by shading on the y-axis) was observed in the signal peptide (red) and translocator domain (yellow), while diversity in sequence and size was seen in the passenger domain (blue) of the proteins. (B) Unrooted phylogram of 24 UpaG translated amino acid sequences. Branch confidence levels are >90% and were determined from 1,000 bootstrap replicates of Neighbor-Joining trees calculated using PHYLIP (21). Taxon IDs represent the locus tags assigned to *upaG* orthologues in each *E. coli* genome sequence (see Table S1). Sequences from commensal and laboratory *E. coli* strains are indicated in blue, from diarrheagenic *E. coli* (DEC) in red and from extraintestinal pathogenic *E. coli* (ExPEC) in green.

Fig 2. *In silico* analysis of UpaG and EhaG homologues. (A) Schematic illustration of the domain organisation of UpaG and EhaG proteins. Indicated are the signal peptide (S.P.), translocator domain (Pfam: YadA), and the localization of the multiple invasin (Pfam: Hep_Hag) and hemagglutinin (Pfam: HIM) motifs within the passenger domain. (B) Multiple sequence alignment of the Hep_Hag repeats and HIM motifs of EhaG and UpaG. The domains were identified by sequence searches against the Pfam (22) and TIGRFAM databases hosted by the Comprehensive Microbial Resource (http://cmr.jcvi.org). Highly conserved residues are indicated in red. (C) Consensus sequence of the EhaG and UpaG Hep_Hag repeats and HIM motifs. Dots, no consensus; lowercase, some consensus; uppercase, high consensus.

Fig 3. EhaG promotes autoaggregation and biofilm formation in *E. coli*. (A) Settling profile of liquid suspensions of *E. coli* strains MS427pBAD (vector control) and MS427pEhaG. Suspensions were prepared from overnight LB cultures supplemented with 0.2% arabinose normalized at an OD_{600nm} of 1. Bacterial autoaggregation is inversely proportional to the optical density of each suspension measured at 600nm over a period of 60 minutes. (B) Biofilm formation by *E. coli* strains MS427pBAD (vector control) and MS427pEhaG following 18 hrs culture in LB medium supplemented with 0.2% arabinose. Biofilm formation was examined in polystyrene 96-well microtitre plates using crystal violet staining.

Bar charts show average absorbance measurements at 590nm ± SEM from three independent experiments. (C) Fluorescent micrographs of continuous flow biofilms formed in glass chambers 18 h after inoculation with GFP-labelled *E. coli* strains (i) OS56pBAD (vector control), (ii) OS56pEhaG, and (iii) OS56pUpaG. Micrographs show representative horizontal sections collected within each biofilm. Shown to the right and below of each individual panel are vertical sections representing the yz-plane and the xz-plane, respectively, at the positions indicated by the red and green lines.

Fig 4. EhaG and UpaG mediate *E. coli* adherence to ECM proteins. ELISA-based assay demonstrating binding of *E. coli* MS427pEhaG (black bars), *E. coli* MS427pUpaG (grey bars), and *E. coli* MS427pBAD (white bars) to collagen (I-V), fibronectin, fibrinogen and BSA. Results represent average absorbance readings at 405 nm + SEM from three independent experiments. The expression of EhaG and UpaG was induced with 0.2% arabinose.

Fig 5. EhaG mediates *E. coli* adhesion to intestinal epithelial cells. (A) Binding efficiency of *E. coli* MS427 containing pBAD, pEhaG or pUpaG to Caco-2 epithelial cell monolayers. Bars represent the average number of adherent bacteria (CFU) per epithelial cell monolayer ± SEM. (B) Competitive adhesion to Caco-2 epithelial cell monolayers of mixed (1:1) bacterial inocula containing MS427green-pEhaG and MS427red-pUpaG. Bars represent average number of each bacterial strain (CFU) per field of view ± SEM. (C) Representative field of view of micrographs used to quantify the number of UpaG- and EhaG-producing adherent bacteria in the competitive Caco-2 epithelial cell adhesion assay. MS427pEhaG cells are tagged with GFP and MS427pUpaG cells are tagged with RFP. The expression of EhaG and UpaG was induced with 0.2% arabinose.

Fig 6. H-NS repression of *upaG* expression in UPEC CFT073. (A) β-galactosidase activity of a chromosomal *upaG*::*lacZ* reporter fusion in CFT073Δ*lac* and CFT073Δ*lac_hns* alone, with pBAD30 (vector control) or pBAD30*hns* (complementation vector). pBAD30 and pBAD30*hns* containing strains were grown in presence of 0.2% arabinose. (B) Curvature plot of the *upaG* promoter sequence. (C) Electrophoretic mobility of the *upaG* promoter sequence. (D) Electrophoretic mobility shift assay of H-NS binding to the *upaG* and *bla* promoter sequences.

Fig 7. Production of UpaG (in CFT073) and EhaG (in EDL933) in a *hns* mutant background. Western blot analysis of whole cell lysates prepared (A) from *E. coli* CFT073 and CFT073*hns* employing a rabbit polyclonal anti-UpaG serum, and (B) from *E. coli* EDL933, and EDL933*hns* using a rabbit polyclonal anti-EhaG serum. The monomeric UpaG and EhaG proteins are indicated; possible oligomeric forms of each protein are indicated by asterisks.

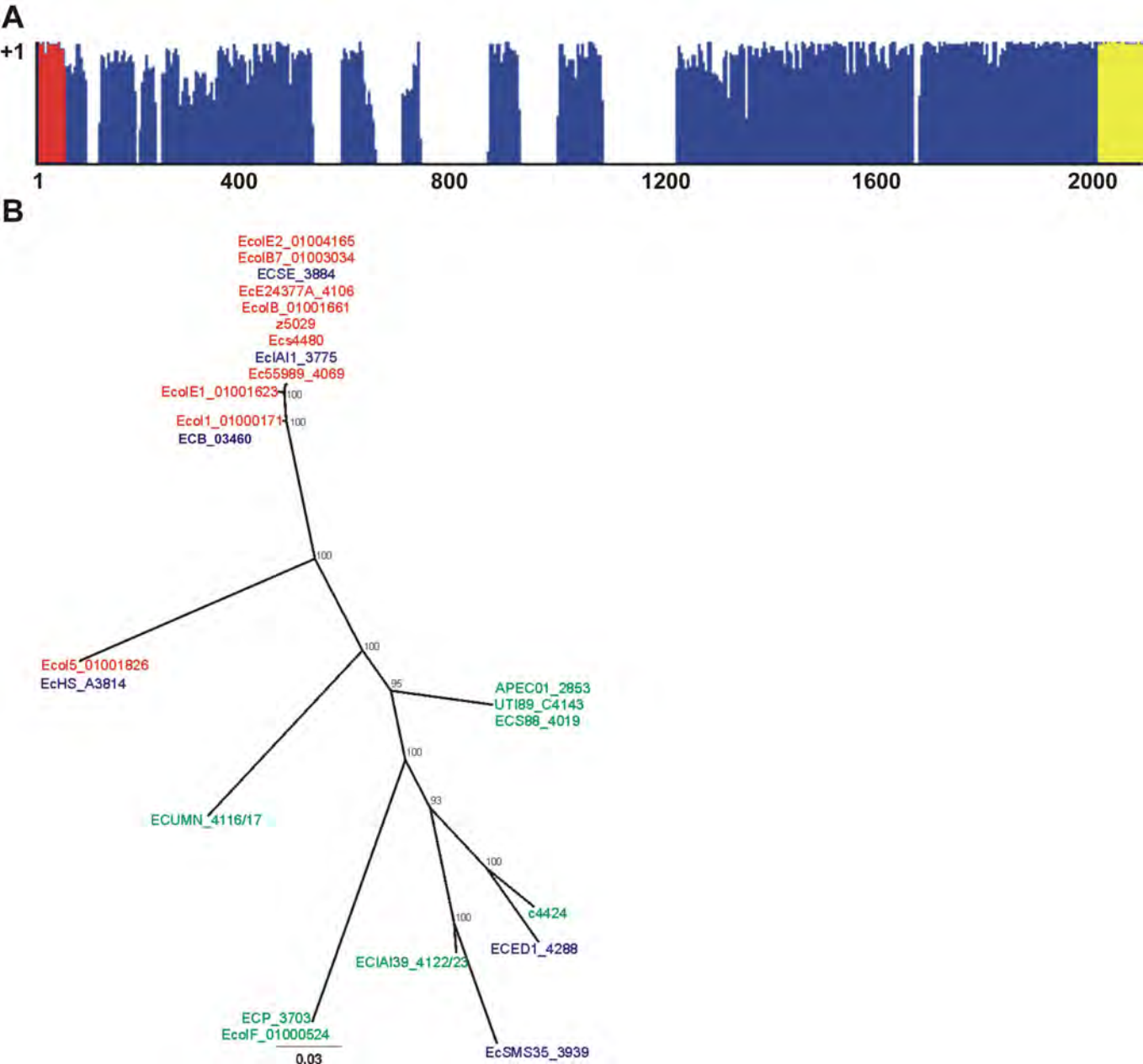
A
+1
1
400
800
1200
1600
2000
B
EcolE2_01004165
EcolB7_01003034
ECSE_3884
EcE24377A_4106
EcolB_01001661
z5029
Ecs4480
EclAI1_3775
Ec55989_4069
EcolE1_01001623
Ecol1_01000171
ECB_03460
Ecol5_01001826
EcHS_A3814
APEC01_2853
UTI89_C4143
ECS88_4019
ECUMN_4116/17
c4424
ECED1_4288
EClAI39_4122/23
ECP_3703
EcolF_01000524
EcSMS35_3939
0.03

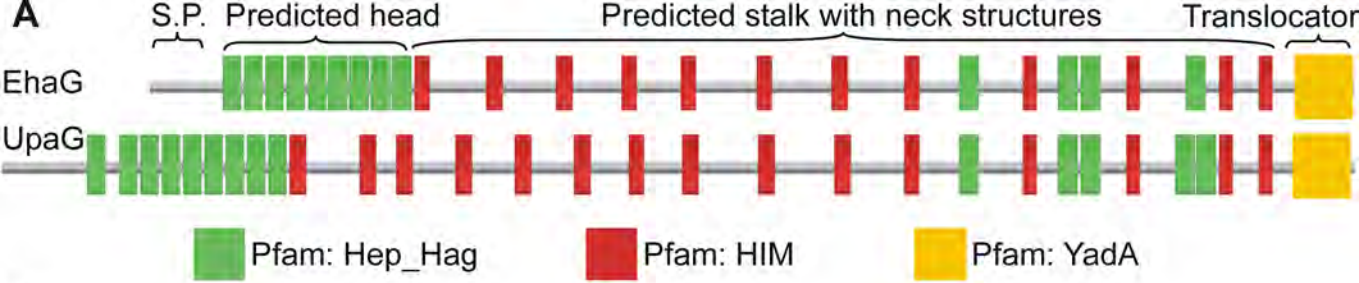

B

EhaG Hep_Hag	UpaG Hep_Hag	EhaG HIM	UpaG HIM
AEGQYSSAIGSKTHAIGGASMAFGVSAI	ATGGASMAFGVSAKAMGDRSVALGASSV	RKIVNVKNGAIKSDSYDAINGSQL	RKIVNMAAGAISNTSTDAINGSQL
SEGDRSIALGASSYSLGQYSMALGRYSK	TNGFTSLAIGDSSLADGEKTIALGNTAK	SVITDVADGTISASSKDAVNGSQL	NKITNVAKGTVSATSTDVVNGSQL
ALGKLSIAMGDSSKAEGANAIALGNATK	AYEIMSIALGDNANASKEYAMALGASSK	SKITNVKDADLTADSTDAVNGSQL	SKITNVTAGNLTAGSTDAVNGSQL
ATEIMSIALGDTANASKAYSMALGASSV	AGGADSLAFGRKSTANSTGSLAIGADSS	SKITNVKDGDLTTGSTDAVNGSQL	SKITNVTAGNLTAGSTDAVNGSQL
ASEENAIAIGAETEA-AENATAIGNNAK	SSNDNAIAIGNKTQALGVNSMALGNASQ	SKITNVILDGTVTATSSDAINGSQL	SKITNVTAGTLTAGSTDAVNGSQL
AKGTNSMAMGFGSLADKVNTIALGNGSQ	ASGESSIALGNTSEASEQNAIALGQGSI	SVITDVADGEISDSSSDAVNGSQL	SKITNVKAGDLTAGSTDAVNGSQL
ALADNAIAIGQGNKADGVDAIALGNGSQ	ASKVNSIALGSNSLSSGENAIALGEGSA	SVITNVANGAISAASSDAINGSQL	SKITNVKAGDLTAGSTDAVNGSQL
SRGLNTIALGTASNATGDKSLALGSNSS	AGGSNSLAFGSQSRANGNDSVAIGVGAA	SIITNVANGSISEDSTDAVNGSQL	SKITNLLAGKISSNSTDAINGSQL
ANGINSVALGADSIADLDNTVSVGNSSL	AATDNSVAIGAGSTTDASNTVSVGNSAT	RQIINVADG---SEAHDAVTVRQL	SVITDVANGAVSSTSSDAINGSQL
AQGVGATAIGYNSVAKGDSSVAIGQGSY	ASGIGATAVGYNAVASHASSVAIGQDSI	RQITNVAAG---SADTDAVNVGQL	SVITNVANGAVSATSNDAINGSQL
AVGTDSLAMGAKTIVNGDKGIGIGYGAY	AVGEDSLAMGAKTIVNGNAGIGIGLNTL	RRITNVAAG---KNATDAVNVAQL	SKITNVAAGDLSTTSTDAVNGSQL
ANALNGIAIGSNAQVIHVNSIAIGNGST	ADAINGIAIGSNARANHADSIAMGNGSQ	TRISNVSAG---VNNNDVVNYAQL	RQIINVADG---SEAHDAVTVRQL
AQGKDSVAIGSGSIAAADNSVALGTGSV	AAADNSVALGTGSVADEENTISVGSSTN		RQITNVAAG---SADTDAVNVGQL
	TKYFKTNTDGADANAQGKDSVAIGSGSI		RRITNVAAG---VNATDAVNVSQL
			TRISNVSAG---VNNNDAVNYAQL

C

```
EhaG Hep-Hag: a.g.n(s/a)iA(i/l)G..s.a.g.ns(v/i)A(l/i)Gn.s.
UpaG Hep-Hag: a.g..s(i/l)A(l/i)G.(n/k)(s/a).a.g..(s/a)(v/i)A(l/i)G..s.

EhaG Him: s(k/v)ITNVa(d/n)G.(i/v)(s/t)..s(s/t)DA(v/i)NgsQL
UpaG Him: s(k/v)ITNVa(d/n)G.(i/v)(s/t)..s(s/t)DA(v/i)NgsQL
```

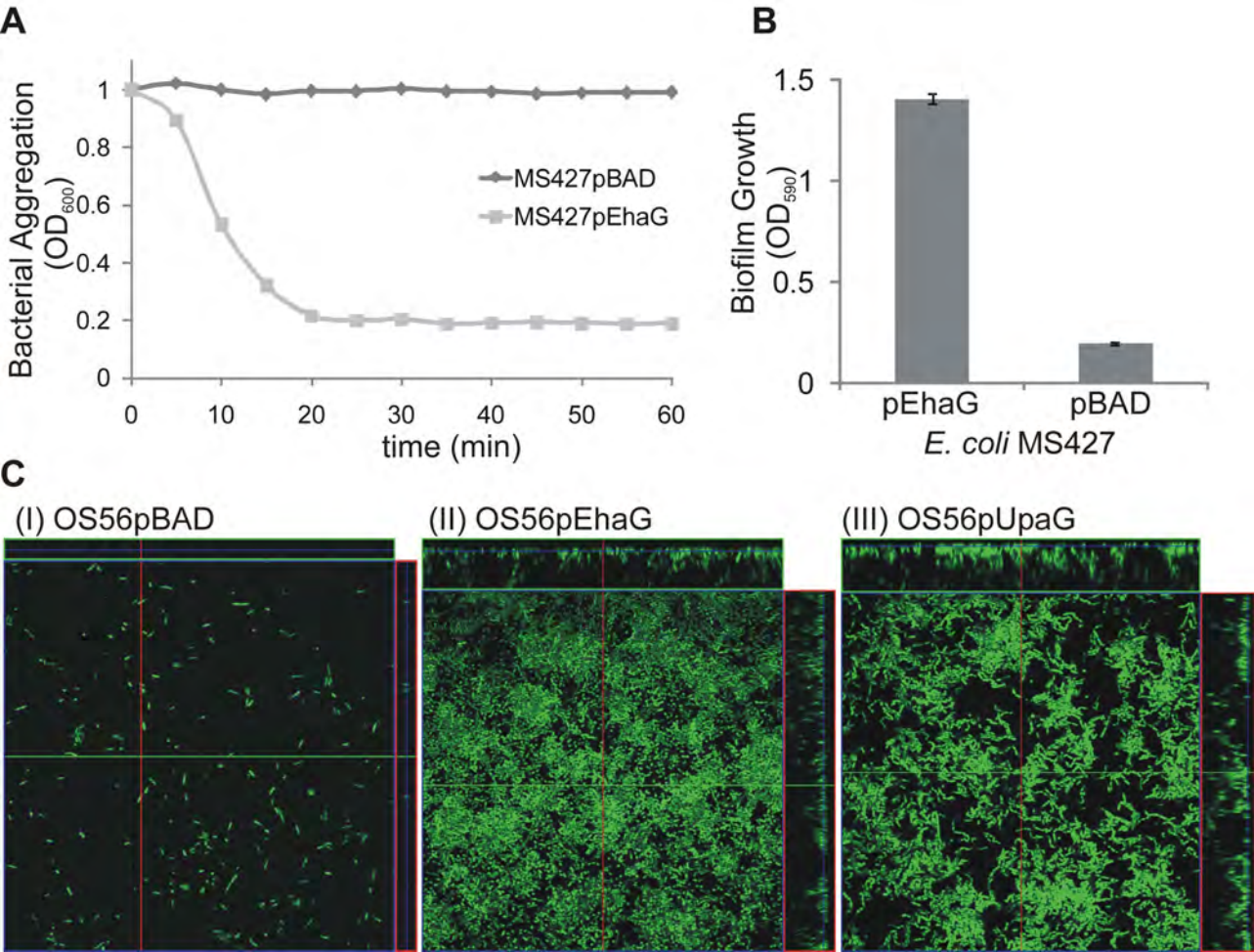
A
Bacterial Aggregation (OD600)
1
0.8
0.6
0.4
0.2
0
0
10
20
30
40
50
60
time (min)
MS427pBAD
MS427pEhaG
B
Biofilm Growth (OD590)
1.5
1
0.5
0
pEhaG
pBAD
E. coli MS427
C
(I) OS56pBAD
(II) OS56pEhaG
(III) OS56pUpaG

Bacterial Adhesion
(OD405)
0
0.1
0.2
0.3
0.4
0.5
0.6
0.7
0.8
pEhaG
pUpaG
pBAD
Collagen I
Collagen II
Collagen III
Collagen IV
Collagen V
Fibronectin
Fibrinogen
Laminin
BSA

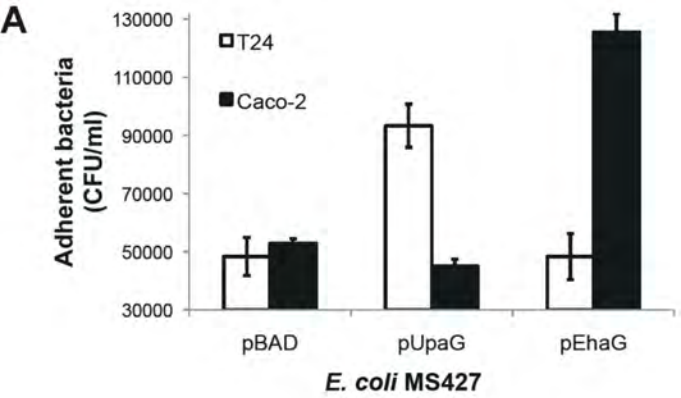
A
130000
110000
90000
70000
50000
30000
T24
Caco-2
Adherent bacteria (CFU/ml)
pBAD
pUpaG
pEhaG
E. coli MS427

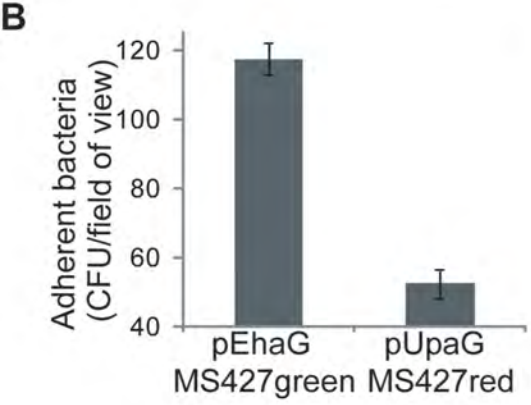
B
120
100
80
60
40
Adherent bacteria (CFU/field of view)
pEhaG
MS427green
pUpaG
MS427red

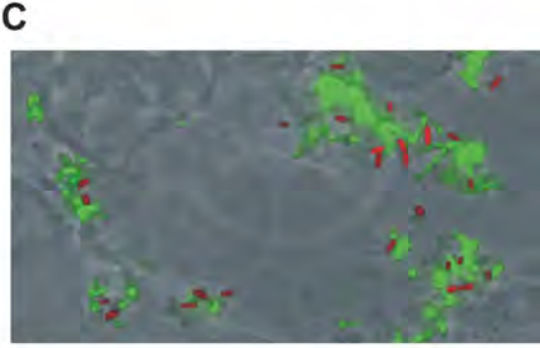
C

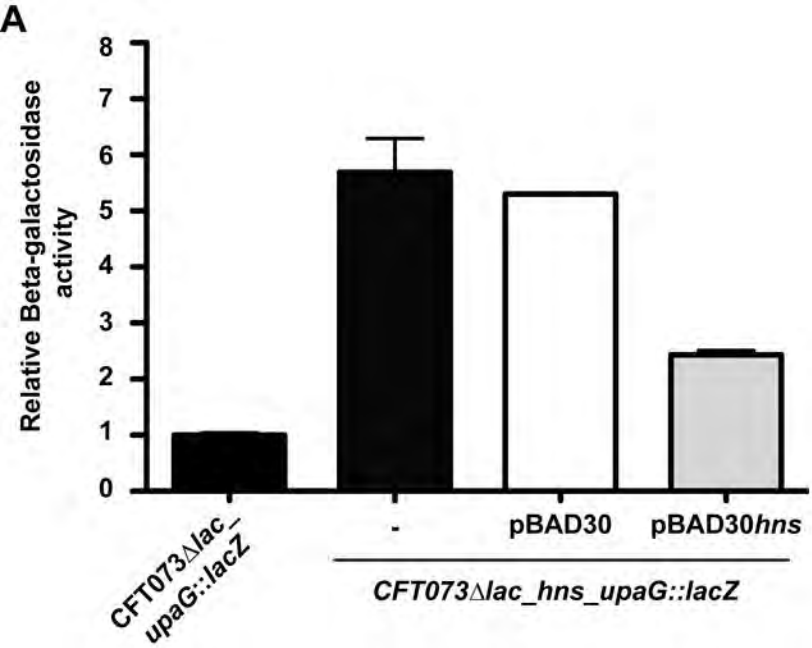
A
Relative Beta-galactosidase activity
8
7
6
5
4
3
2
1
0
CFT073Δlac_ upaG::lacZ
-
pBAD30
pBAD30hns
CFT073Δlac_hns_upaG::lacZ

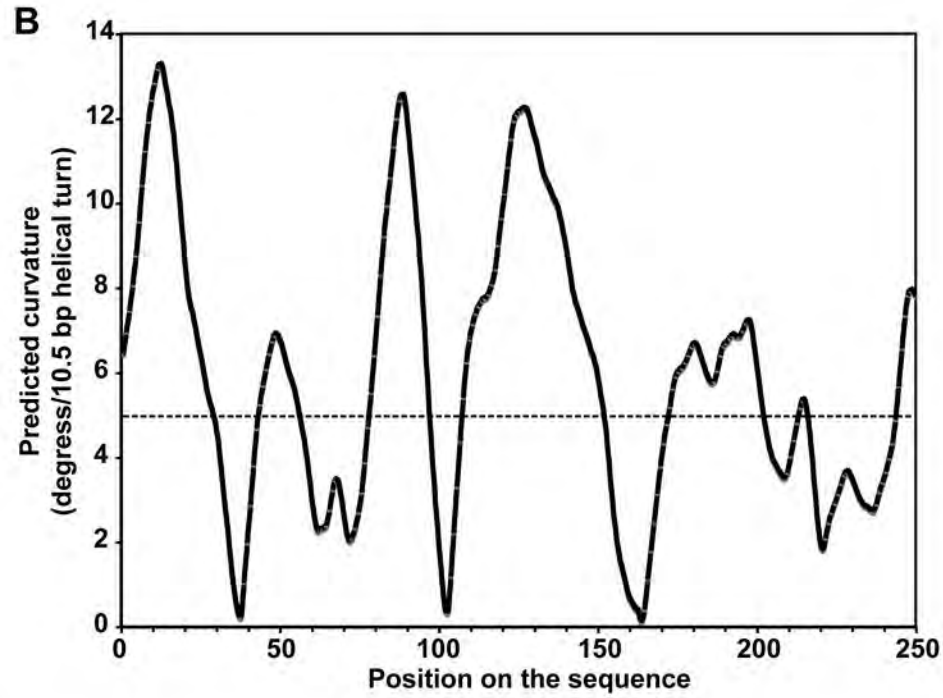
B
Predicted curvature (degress/10.5 bp helical turn)
14
12
10
8
6
4
2
0
0
50
100
150
200
250
Position on the sequence

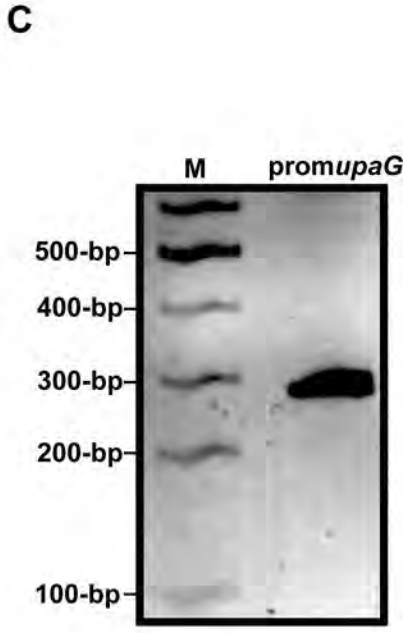
C
M
promupaG
500-bp
400-bp
300-bp
200-bp
100-bp

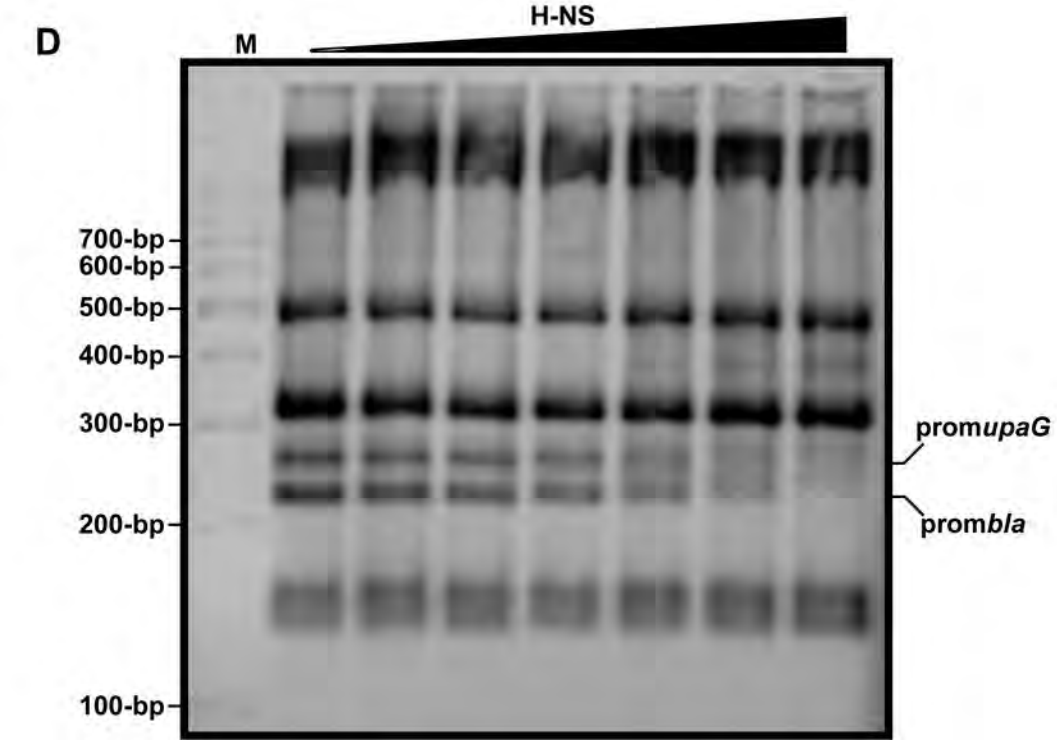
D
M
H-NS
700-bp
600-bp
500-bp
400-bp
300-bp
200-bp
100-bp
promupaG
prombla

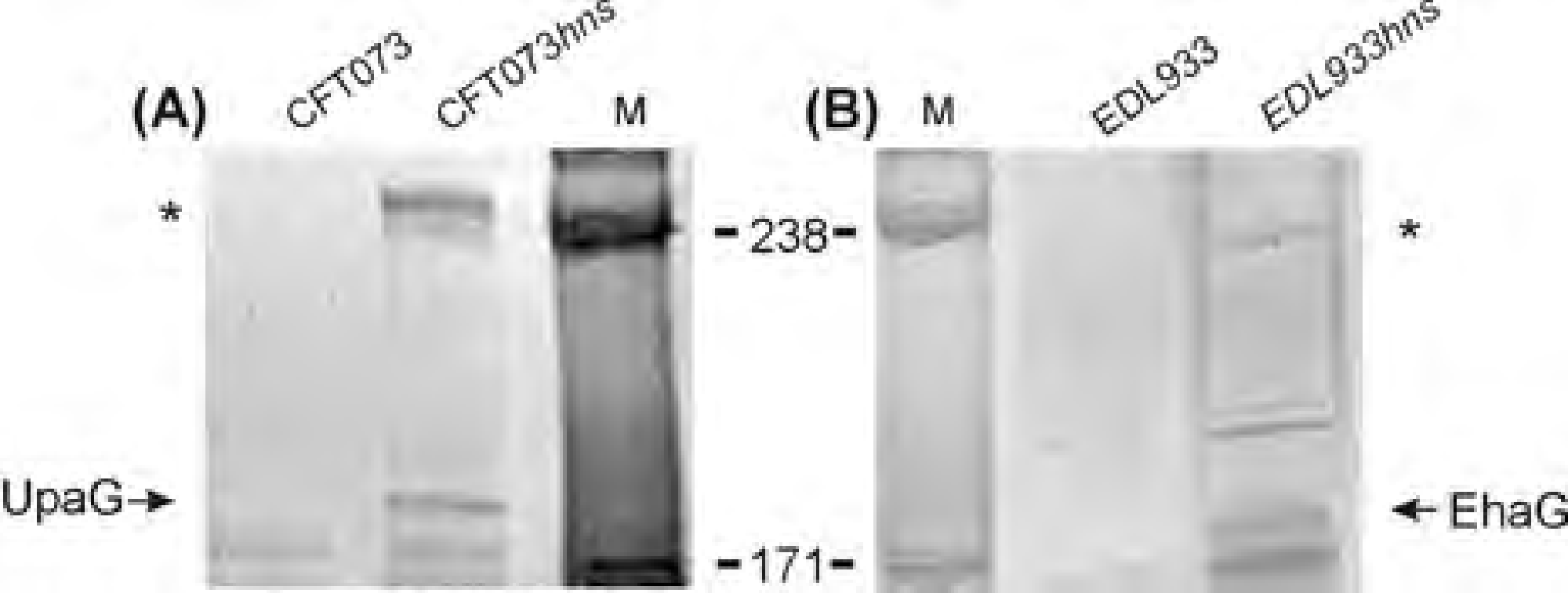
(A)
CFT073
CFT073hns
M
*
UpaG
238
171
(B)
M
EDL933
EDL933hns
*
EhaG